UNIVERSITY OF CALIFORNIA, SAN DIEGO

A New Numerical Simulation Model for Standard Effective Temperature

A thesis submitted in partial satisfaction of the
requirements for the degree Master of Science

in

Engineering Sciences (Mechanical Engineering)

by

Jipeng Fan

Committee in Charge:

Professor Jan Kleissl, Chair
Professor Carlos F. Coimbra
Professor Eugene R. Pawlak

2015

The thesis of Jipeng Fan is approved, and it is acceptable in quality and form

For publication on micro film and electronically:

_____

_____

_____

Chair

University of California, San Diego

2015

DEDICATION

To my parents, Xiangjun Fan and Yun Guo

TABLE OF THE THESIS

LIST OF FIGURES

ACKNOWLEDGEMENTS

First and foremost, I would like to acknowledge Professor Jan Kleissl for his support as the chair of my committee with my most sincere gratitude. Through multiple drafts and directional guidance, his help has proved to be invaluable. I greatly enjoyed working in his Lab.

I would also like to acknowledge Negin Nazarian from Center of Energy Research, without her data and help on revising there can be no research to speak of. Data from her research is used as a baseline of this study.

In addition, I would like to thank my office mates, Abdullah Habib and Zachary Pecenak, for their interest of this study.

Chapter 2, Chapter 3, Chapter 4 and Chapter 5, in part, is a reprint of the material as it appears in "A New Numerical Simulation Model for Standard Effective Temperature", Jipeng Fan, Negin Nazarian, Jan Kleissl. The dissertation author was the primary investigator and author of this paper.

ABSTRACT OF THE THESIS

A New Numerical Simulation Model for Standard Effective Temperature

by

Jipeng Fan

Engineering Sciences (Mechanical Engineering)

University of California, San Diego, 2015

Professor Jan Kleissl, Chair

This paper introduces a new method to calculate the spatial variation of the Standard Effective Temperature (SET) in a three-dimensional idealized urban area. The SET is a thermal comfort index that describes human sensation in the urban environment. It derives the SET by modeling the mean radiant temperature, urban area visibility, building shade area and two-nodes SET model. The major novelty of this paper is a matrix-based model for the SET. Spatial SET prediction is evaluated at the pedestrian level (1.5 m from the ground) in an idealized urban area in a clear summer day of San Diego California CFD simulations of flow field coupled with heat transfer used for obtaining urban surface temperature, wind velocity and air pressure.

This study reveals that SET has a high variability in the horizontal directions within a small urban area. This method is still under development. The next step is to complex the idealized urban model to a real urban model and compares simulation results with the measurement data.

1. Introduction

1.1. Background

Urbanization is a population shift from rural to urban areas, and the ways in which society adapts to the change. It predominantly results in the physical growth of urban areas. A UN report [1] shown that, by 2008, urban population has exceeded rural population for the first time in human history. The report also predicts that, by 2050, 7 out of every 10 people will live in an urban area.

This fast grown urban population rate could cause a series of social and environmental problems. Urban Heat Island (UHI), which refers to a phenomena that cities are significantly warmer than surrounding rural area, is shown to be exacerbated with increased urban population [2–5]. It is shown that the urban heat island is directly responsible for morbidity rate and public health concerns in densely built areas [6–8]. Accordingly, in order to evaluate the human response to the urban thermal fields, the American Society of Heating, Refrigerating, and Air-Conditioning Engineers (ASHRAE), has introduced methodologies to comprehensively express human sensation in the thermal environment, or better put thermal comfort. Thermal comfort is significant to human health [9] and received wide attention among HVAC design engineers for indoor building environment. There are multiple thermal comfort index, each of them is evaluated on different human body model. In 1986, Gagge [10] developed a thermal comfort index called standard effective temperature (SET), based on a two-nodes body model. SET is a comprehensive metric that integrates the influences of air temperature, wind velocity, humidity and radiation on the thermal sensation and has applications in thermal environment engineering both for indoor and outdoor, as it successfully relate all the environmental variables with a person's

thermal experience. In this current paper, we picked the SET as study object because it is one of the most common thermal comfort index [11].

1.2. Method

One of the most common SET study methods is calculating SET in a real urban area, using empirical data. This method has been broadly used in cities around the world, such as Tokyo [12], Osaka [13], Barcelona [14], Chennai [15]. However, this method is lacking accuracy (highly measurement results demand) and has ignored the change of thermal environment from urban geometry. With the increase in the extreme events around the world [16, 17] and the demand for energy sustainable cities, more accurate methods of evaluating thermal com- fort is also needed, which motivates the improvement of SET calculation method. The new method should be able to predict the SET in order to give better energy saving idea to architects from architectural planning stage. One of the most important and complicated variables for SET calculation is mean radiant temperature (MRT), which is the uniform temperature of an imaginary enclosure in which the radiant heat transfer from the human body is equal to the radiant heat transfer in the actual non-uniform enclosure. Currently there are many online calculators, such as CBE Thermal Comfort Tool [18], that calculate the SET using a given value of MRT, assuming that MRT can be easily evaluated by using a bolometer. However, accurate calculation of MRT in a complex three-dimensional geometry adds further complication to SET prediction in outdoor environments. Several studies are focused on the MRT simulation methods in outdoor environments, in-cluding ENVI-met 3.1 [19], Rayman 1.2 [20], CityComfort+ [21] and SOLWEIG 2.2 [22]. But each of them has limitations on accuracy or spatial prediction ability. ENVI-met is hard to use. Topography and vegetation are had to be transferred manually to pixels.

It is also highly computationally demanding for common desk top computers. Some papers even indicate that ENVI-met is questionable when compare results with measurement data [23]. Rayman is more user friendly but it cannot simulate the MRT at multi-points per time and it cannot account for reflected solar radiation [24]. SOLWEIG is lacking accuracy on radiation modeling [22]. CityComfort+ is under development and cannot be applied for non-constant long wave radiation from the sky.

In this study, a new numerical model to predict the spatial distribution of standard effective temperature is introduced and sensitivity of this variable to several design elements are evaluated. CFD simulations done by Nazarian et al [25] is used for obtaining detailed parameters in the three-dimensional idealized urban area, such as air and facet temperatures, wind velocity and air pressure, further explained in Section 2. The simulation is performed in a clear summer day (June 22nd) in San Diego (32.867 N, 117.133 W), California, USA. SET calculation is done mostly on the pedestrian level (1.5 meters). A improved model of SET treats every surface in the urban area, such as ground and building walls, as a matrix. This matrix based model combined with several related algorithms are considered as one of the major improvement of this work. It gives a more accurate 3D special SET plots and a meticulous calculation to the MRT, Shown in section 3, a spatial distribution of SET is presented as varied with time and wind direction. Conclusion is shown in section 4. By calculating the SET, this paper has completed a whole process of thermal comfort simulation (from urban modeling, CFD simulation to MRT modeling, SET calculation) by combining with previous research [25]. We are hoping this methodology can combine with more realized 3D urban model in future and predict thermal comfort to give better suggestion to urban planning

2. Thermal Comfort Theory

The SET is a comfort index that was developed based upon a dynamic two- node model of the human temperature regulation, each node represents body skin and body core. Body core node represents metabolism system and all changes inside the body. Body skin represents skin, which including perspiration system, and clothes.

2.1. Body Surface Area

The skin surface is the boundary between human body (body skin) and surrounding environments. The heat exchange between these two is happened by the radiation, convection and evaporation. The heat of body core, produced by metabolism, reaches this boundary by blood flow. And then the evaporative cool- ing, between body skin and surrounding external environment, is supported by secretion of perspiration on the boundary surface. This process could be effected by both external thermal environment and internal regulatory processes [26]. The most commonly used measure of body surface area, originally represented by Dubis and Dubois [27]

$$A_D = 0.202m^{0.425}l^{0.725} \quad (1)$$

where A_D is Dubois surface area, m^2. m is body weight, kg. l is body height(m). A correction factor $f_{cl} = A_{cl}/A_D$ must be applied to the heat transfer terms from the skin to account for the actual surface area A_{cl} of the clothed body [28].

2.2. Skin Temperature

Skin temperature is one of the major variables of the two-node SET system. It is a signal of temperature sensation to the external thermal environments, both in warmth and cold environment, and independent from this man's activity. Figure 1 has shown that skin temperature distribution of the whole body is not uniform. Gagge [26] has proved

that people will feel more uncomfortable if skin temperature distribution is more different. However, with the two-nodes model, skin temperature distribution could not be considered. In this paper, skin temperature is assumed to be uniform and represented by the body skin node.

2.3. Core Temperature

Hardy[29] and Gagge [30] indicates that activities (mostly metabolism) pro- duce and release energy into the body core as heat. The self-regulation system of human body would regulate the core temperature to be a constant, which can maintain uniform over the body. Illustration of typical core and skin temperature shown as Figure 1.

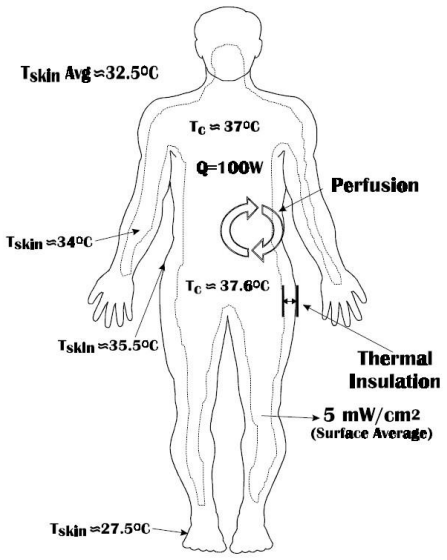

Figure 1: Schematic representation of temperature distribution and heat transfer for an adult human.

2.4. Skin Thermal Conductivity

Skin thermal conductivity is considered to be highly dependent on skin blood flow. Its value change significantly along body age, gender and activity level [28]. Vendrik [31] indicated a determination of an average thermal conductivity to be between 0.293 and 0.322 W/(mk). This value has been commonly used in relative studies. In this current

study, skin thermal conductivity is assumed to be 0.309 as constant.

2.5. Sweating

Human body has ability to self-regulate the evaporative cooling by sweating. Sweating is temperature stimuli from skin and core temperature. Each skin and core temperature represents local controls and central controls. In this paper, sweating is assumed to be free to evaporate from skin surface and the sweating rate is assumed to be constant because metabolism level of human body remains same. This assumption allows sweating rate not become to a uncomfortable process [26].

2.6. Clothing Area Factor

Clothing area factor, present as a rate of cloth covered body area to total body surface area, is considered to be one of the major variables to human body heat loss because it can effect both radiation and conduction. A typical clothing heat transfer analysis requires clothing area factor to be known. The most effective method of measuring clothing area factor is photographic method [32]. However, [28] provides form which contains clothing area factors for each kind of typical cloth ensembles. In this research, we are analyzing for a motionless person standing in summer (June 22nd) urban area with walking shorts, short-sleeved shirt (typical summer wearing). Relative clothing surface area is $f_{cl} = 1.1$ [28].

2.7. Clothes Temperature

The following equation, available from [28], is a empirical formula of cloth temperature. It is originally obtain by Fanger [32]. Fanger has made a basic assumption for this equation which is all sweat generated is evaporated. It is proved to be effective for normal clothing with normal activity level.

$$t_{cl} = 35.7 - 0.0275(M - W) - R_{cl}(M - W) - 3.05[5.73 - 0.007(M - W) - p_a] + 0.42[(M - W) - 58.15] + 0.0173M(5.87 - p_a) + 0.0014M(34 - t_a) \quad (2)$$

2.8. Radiative Heat Transfer Coefficient

Radiant heat exchange is known as a major heat exchange method of human which significantly effect thermal comfort. It can be expressed in terms of the Stefan-Boltzman law. A equation of linearized radiative heat transfer coefficient can be found in ASHRAE HANDBOOK [28]

$$h_r = 4\epsilon\sigma\frac{A_r}{A_D}(273.2 + \frac{t_{cl} + T_r}{2})^3 \quad (3)$$

T_r indicates mean radiant temperature. In this study, we take the ratio of effective radiation area of body to body surface area A_r/A_D as 0.73 [33]. Typically emissivity σ is about 0.95.

2.9. Convective Heat Transfer Coefficient

Convective heat transfer describes heat exchange by air movement in the external thermal environment. It is a function of subject's posture, clothes and wind velocity. Seppanen et al [34] introduce an empirical equation of convective heat transfer coefficient, which simplified the convective heat transfer coefficient to be a function of wind velocity for different typical clothes and subject's posture.

$$h_c = 8.6v^{0.53} \quad (4)$$

This heat transfer coefficient was evaluated at or near 101.33 kPa. Considering pressure difference in the domain, a valid convective heat transfer coefficient should involve pressure difference in the calculation, which is

$$h_{sc} = h_c(\frac{p_t}{101.33})^{0.55} \quad (5)$$

where h_{sc} is corrected convective heat transfer coefficient. pt is local atmosphere pressure.

2.10. Evaporative Heat Transfer Coefficient

Sweat and other liquids evaporate from body skin and release heat to the external environment. This process could be change with cloth area factor, skin temperature and pressure. Evaporative heat loss is considered to be important to the human body heat balance. Oohori et al [10] and Wookcock [35] introduced the Lewis relation, which is the main method of calculating the evaporative heat transfer coefficient.

$$\text{LR} = 15.15\frac{t_{sk}}{273.2} \quad (6)$$

$$\text{LR} = \frac{h_e}{h_c} \quad (7)$$

where LR is the Lewis Ratio. If considering the pressure difference, especially when the atmospheric pressure is significantly different from the reference value (101.33 kPa), a correct value of corrected evaporative heat transfer coefficient should be considered, which can be obtained from Equation 6, 7 and 8

$$h_{ec} = h_e(\frac{101.33}{P_t})^{0.45} \quad (8)$$

2.11. Evaporative Heat Loss From Skin

Evaporative heat loss E_{sk} from skin depends on the skin wetness, water vapor pressure at skin and ambient temperature, evaporative heat transfer resistance of clothing area and evaporative heat transfer coefficient. The equation gave by [28]

$$E_{sk} = \frac{w(P_{sk} - P_a)}{R_{cl} + \frac{1}{f_{cl}h_e}} \quad (9)$$

where *w* is skin wetness. P_{sk} is water vapor pressure at skin, normally assumed to be the saturated water vapor at t_{sk} . P_a is water vapor pressure at ambient air. R_{cl} is evaporative heat transfer resistance of clothing layer. $h_e = l_r \times h_{sc}$ is evaporative heat transfer coefficient. Skin wetness is the ratio of the actual evaporative heat loss to the maximum possible evaporative heat loss E_{max} with the same conditions and a completely wet skin (w = 1). With no regulatory sweating, skin wetness caused by diffusion is approximately 0.06 for normal conditions. Most simulations [36] reveal that skin wetness is difficult to exceed 0.8. Azer [37] recommends 0.5 as a practical upper limit to the skin wetness. In this study, skin wetness with no regulatory sweating was calculated by following equations [28]

$$w_{rsw} = \frac{E_{rsw}}{E_{max}} \tag{10}$$

Evaporative heat loss by regulatory sweating is directly proportional to the rate of regulatory sweat generation.

$$E_{rsw} = \dot{m}_{rsw} h_{fg} \tag{11}$$

where h_{fg} is heat of vaporization of water. $\dot{m}_{rsw}$ is rate at which regulatory sweat is generated, which can be found in Nigel as Taylor (2013).

2.12. Internal Heat Production

Internal heat production is produced by the oxidation processes in the human body per unit time. Metibolic rate M might be effected by the external mechanical power W, but it always be considered to convert to internal body heat H, the equation shown as follow

$$\mathrm{M} = \mathrm{H} + \mathrm{w} \tag{12}$$

Introducing the definition of external mechanical efficiency

$$\eta = \frac{W}{M} \tag{13}$$

which gives $\mathrm{H} = \mathrm{M}(1-\eta)$.

2.13. Intrinsic Insulation

Methods to determine clothing insulation are measurements on heated mannequins [38, 32]. For most engineering work, estimation can be built on these following equations.

$$I_{cl} = \frac{1.33}{M - W + 0.74} - 0.095 \tag{14}$$

Intrinsic insulation of the clothing layer

$$I_a = \frac{1}{f_{cl} h} \tag{15}$$

In this research, since we assume the analyzed subject is wearing walking shorts, short-sleeved shirt (typical summer clothes). Cloth area and intrinsic insulation factor are $\mathrm{f_{cl}} = 1.1$ and $\mathrm{I_{cl}} = 0.36$, which suggested by McCULLOUGH and Jones [38].

2.14. Mean Radiant Temperature

Mean radiant temperature (MRT) is a key variable in thermal calculation for the human body. It represents the radiative effect from external thermal environment to human body. There are multiple existed methods to calculate the mean radiant temperature. Huang [21] introduces a method of calculation which considering all the types of radiation, both including short wave and long wave radiation

$$T_{mrt} = \sqrt[4]{\frac{1}{\sigma}(a_p E_{sol} F_{sol\to p} + \varepsilon_{sky} E_{sky} F_{sky\to p} + \varepsilon E_{urb} F_{urb\to p})} \tag{16}$$

where σ is Stefan-Boltzmann constant, 5.67×10−8. a_p is absorption coefficient of solar radiation for a person (standard 0.7). $\mathrm{E_{sky}}$ is emissivity of the sky. $\mathrm{E_{urb}}$ is

emissivity of solid surfaces. E_{sol} is solar radiation intensity. E_{sky} is long wave radiation intensity of the sky. $F_{sol\rightarrow p}$ is view factor between the short wave sources and the subject. $F_{sky\rightarrow p}$ is view factor between the visible sky and the subject. $F_{urb\rightarrow p}$ is view factor between urban surfaces and the subject

$$T_r = (\frac{S_{str}}{\varepsilon_p \sigma} - 273.15)^{1/4} \quad (17)$$

Algorithms for view factor calculating can be found in [39] [39] and [40].

2.15. Operative Temperature

The SET is a function of temperature. In order to simplify the calculation, a new index was built to combine the mean radiant and ambient air temperatures, each weighted by their respective heat transfer coefficient

$$t_o = \frac{h_r T_r + h_{cc} t_a}{h_r + h_{cc}} \quad (18)$$

$$\mathrm{h} = h_r + h_{cc} \quad (19)$$

After the operative temperature, a standard operative temperature was built up for combining more variables. It is defined as the uniform temperature of a still air enclosure. Thus, by definition [41]

$$t_{so} = \frac{h_p t_o}{h_{sp}} + (1 - \frac{h_p}{h_{sp}}) t_{sk} \quad (20)$$

where h_{sp} is the standard heat transfer coefficient, W/m^2, $h_{sp} = h_p + h_r$;

2.16. Water Vapor Pressure

The water vapor pressure is the pressure where water vapor is in condensed state and thermodynamic equilibrium. As for other substances, water vapor pressure is a function of temperature and can be determined with Clausius-Clapeyron relation.

$$\mathrm{P} = \exp(20.386 - \frac{5132}{T}) \tag{21}$$

where P is the water vapor pressure, T is temperature. Standard operative vapor pressure is defined as the uniform vapor pressure $p_{so}$of a still air enclosure at t_{so} in which the evaporative heat loss from the skin surface would be the same as in the test environment [41].

$$p_{so} = \frac{h_e p_a}{h_{es}} + (1 - \frac{h_s p}{h_{es}} p_{ssk}) \tag{22}$$

and

$$h_{es} = h_e(\frac{101.33}{p_a})^{0.45} \tag{23}$$

Insensible heat transfer coefficient [28], defined as $h_e = 1/(R_{ea} + R_{ecl})$, refers to heat loss rate that does not result in an increase in the temperature of the surrounding air. This equation is assumed that the latent heat of evaporation occurs on the skin surface, and the passage of water vapor be released to the ambient environment is a function of the air vapor resistance R_{ea} and the clothing layers vapor resistance R_{ecl}. In our case, we use insensible heat transfer as the simulation condition because we are assuming only one person standing in the urban area, no significant temperature increasing in the area by human activities. R_{ea} and R_{ecl} are both available from ASHRAE HANDBOOK 2009 [28].

2.17. Heat Balance

Figure 1 shows the thermal interaction of the human body with the external thermal environment. The total metabolic rate within the body is the metabolic rate required for the person's activity plus the meteoric level required for shivering. M-W is transferred to the environment through the skin surface, this causing the body's temperature to rise or fall.

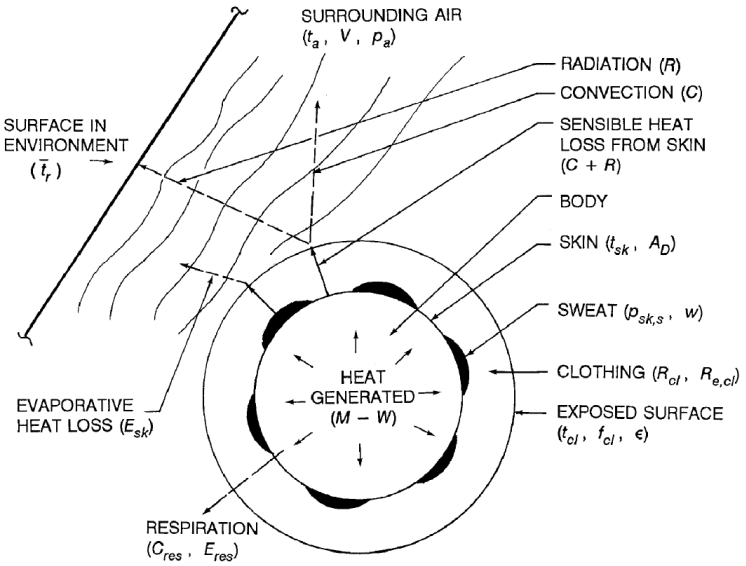

Figure 2: A two node concentric shell model of man and his environment

Heat dissipates from the body to the immediate surroundings by several modes of heat exchange. Since the purpose of the thermo-regulatory system of the body is to maintain an essentially constant internal body temperature, it can be assumed that for long exposures to a constant (moderate) thermal environment with a constant metabolic rate a heat balance will exist for the human body. The heat balance for this condition is

$$\begin{aligned} \mathrm{M} - \mathrm{W} &= q_{sk} + q_{res} + S \\ &= (C + R + E_{sk}) + (C_{res} + E_{res}) + (S_{sk} + S_{cr}) \end{aligned} \tag{24}$$

where M is rate of metabolic heat production. W is rate of mechanical work accomplished. q_{sk} is total rate of heat loss from skin. q_{res} is total rate of heat loss through respiration. C+R is sensible heat loss from skin. E_{sk} is total rate of evaporative heat loss from skin. C_{res} is rate of evaporative heat loss. Eres is rate of evaporative heat loss from respiration. S_{sk} is rate of heat storage in skin compartment. S_{cr} is rate of heat storage in core compartment.

2.18. Standard Effective Temperature

The standard effective temperature is defined as the equivalent temperature of an isothermal environment at 50 percent RH where a subject, while wearing clothing standardized for the activity concerned, would have the same heat stress (skin temperature, t_{sk}) and thermo-regulatory strain (skin wetness, w) as in the actual test environment. Isothermal environment refers to the environment at sea level, in which the air temperature is equal to the mean radiant temperature, and the air velocity is zero. Take H_{sk} as the heat loss from skin, that is the thermal load of skin, then it can be expressed as [41]

$$H_{sk} = h_{sp}(t_{so} - SET) + wh_{se}(p_{ssk} - 0.5p_{SET}) \quad (25)$$

where h_{se} the standard evaporative heat transfer coefficient,W/m^2; w the fraction of the wetted skin surface; p_{ssk} the water vapor pressure at skin, normally assumed to be that of saturated water vapor at t_{sk} , kPa. p_{SET} the saturated water vapor pressure at SET, kPa. In this study, we are analyzing standard effective temperature in a stable state, and there will be no significant heat storage within the body. Therefore, H_{sk} is assumed to be zero.

Chapter 2, Chapter 3, Chapter 4 and Chapter 5, in part, is a reprint of the material as it appears in "A New Numerical Simulation Model for Standard Effective Temperature", Jipeng Fan, Negin Nazarian, Jan Kleissl. The dissertation author was the primary investigator and author of this paper.

3. Model Description

3.1. CFD Simulation

CFD simulation of the flow field and heat transfer in a 3D idealized configuration by [25] is used to obtain pressure, velocity and temperature data in the street canyon. Figure 3 shows the simulation configuration where the flow passes over a matrix of 3x3 building with aspect ratio (H/W) of 1. The simulation is done for a representative coastal urban weather station in southern California (San Diego, 32.867 N, 117.133 W). The Reynolds Averaged Navier Stokes (RANS) equations was solved with k-epsilon realizable model for turbulence modeling, with standard wall function for near wall treatments. Refer to [25] for more information.

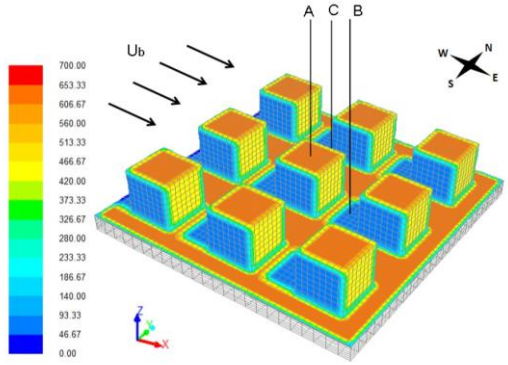

Figure 3: Overview of idealized three-Dimensional urban geometry [25]

3.2. Matrices Based Urban Model

All the ground surface and building surfaces in the urban area were represented by matrices. Column and row in a matrix donated coordinate position of elements. One single building surface matrix represents a extension of building's side surfaces temperature. Four building's side surfaces spread out and shown a one single building surfaces matrix (Figure 5 and 6). MATLAB 2013a, as a successful matrix calculation solver, was used in the matrix model setup. All the four sides of surface of a building expand to one single matrix. Column and row of matrix donate coordinate position of

the element. Each element is used to contain one type of data. Ground matrix and building surface matrix are shown below.

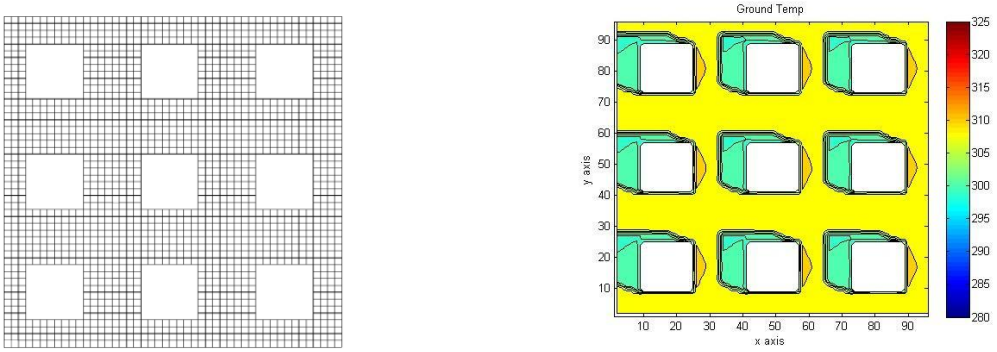

Figure 4: Ground mesh description and matrix of temperature

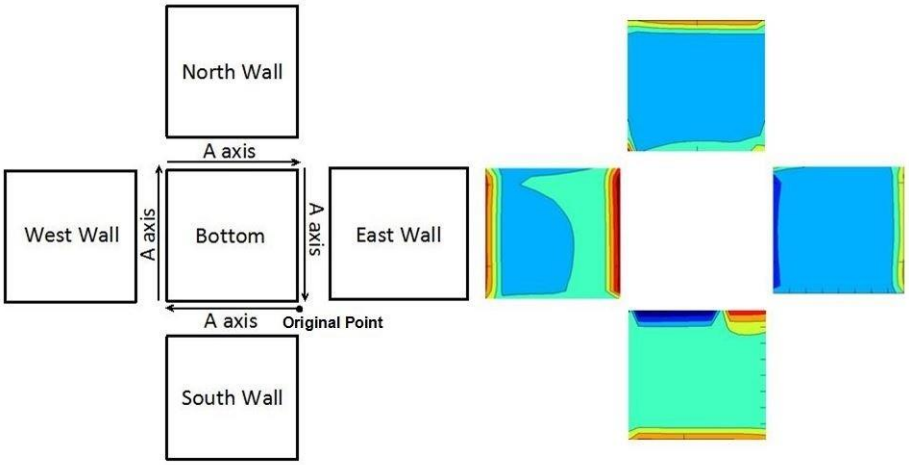

Figure 5: Expanded wall surface matrix

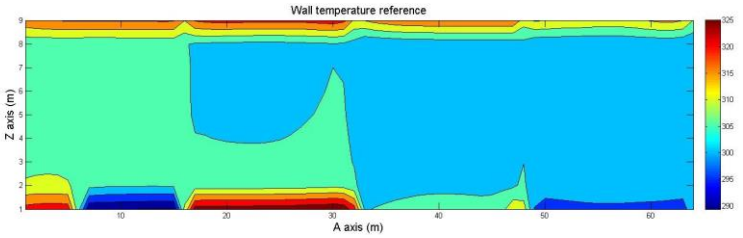

Figure 6: Expanded wall surface temperature

3.3. Mean Radiant Temperature Model

Radiation on the thermal sensation is represented by mean radiation temperature (MRT), which is the uniform temperature of an imaginary enclosure in which radiant heat transfer from the human body is equal to those in the actual non-uniform enclosure. MRT is one of the most important variables to the human thermal comfort in an outdoor urban space. It is commonly used as the composite mean temperature of the body's radiant environment. There are multiple methods to modeling the MRT. It can be estimated by combining the measurements of the globe temperature, air temperature and air velocity. Alfano et al [42] showed many different kinds of typical measurement methodologies to the MRT and re- ported accuracy levels. However, since we want to predict the SET in this paper, no measurement data is available. Jianxiang Huang [21] introduces a method to simulate spatial variation of MRT. He derives the MRT by modeling three primary components of radiation fluxes: short wave radiation (diffuse, direct and reflect), atmospheric long wave radiation and long wave radiation from urban surfaces. Each components weighted by their view factors. The formula shown below

$$T_{mrt} = \sqrt[4]{\frac{1}{\sigma}(a_p E_{sol} F_{sol\to p} + \varepsilon_{sky} E_{sky} F_{sky\to p} + \varepsilon E_{urb} F_{urb\to p})} \tag{26}$$

First term inside square root represents shortwave radiation. Second term is atmospheric long wave radiation. Third term is long wave radiation from urban surfaces.

3.3.1. Short wave Radiation

Short wave radiation, also known as solar radiation, donates a sum of intensity of direct solar radiation, diffuse solar radiation and reflect radiation. Direct solar radiation donates the part of solar radiation radiated from sum and traveling on a

straight line from sun to the surface of earth without any reflection and diffusion. Direct solar radiation only impact in sunlit area. After entered atmosphere, sunlight has been scattered by air molecules or other particles in the air but part of the sunlight still arrives to the surface of the earth, which is known as diffuse solar radiation. Sunlight has been reflected off when it made down to the surface of earth, which is called reflect radiation. To simulate solar radiation in the idealized urban area we analyzed, a demonstrated solar ray-tracing algorithm, ANSYS Fluent ray-tracing algorithm, is used in this study. All three solar radiation types can be calculated from the ANSYS Fluent ray-tracing algorithm.

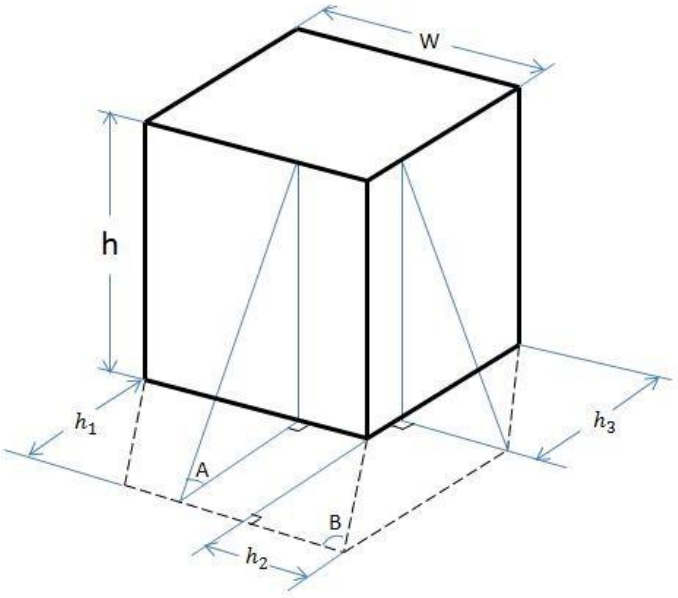

Figure 7: Shadow model description

Diffuse radiation is often considered to be isotropic (ie. uniformly distributed over the sky dome) [43–45]. Shown in Figure 21, reflected radiation is only a small proportion to the total radiation. Therefore, this paper ignores the difference of distribution of reflected radiation and treats both of diffuse and reflect radiation as uniform. However, the direct solar radiation only occurs in sunlit area and it is the most dominant

component to the total solar radiations. Therefore, it is important to find out where the sunlit area is (ie. find out where shade area is). The sunlit area can be modeled by the following formulas. Description shown in Figure 7, break lines donate edge of shade and sunlit:

$$\begin{aligned} \mathrm{A} &= \operatorname{atan}\left(\frac{x}{y}\right) \\ H_1 &= \frac{h}{\tan(A)} \\ \mathrm{B} &= \operatorname{atan}(\frac{y}{z}) \\ H_2 &= \frac{H_1}{\tan(B)} \\ H_3 &= \frac{H_2}{\tan(90-B)} \end{aligned} \tag{27}$$

where x, y, z are solar beam vector (available from ANSYS Fluent ray-tracing algorithm)

An shade modeling example shown as below:

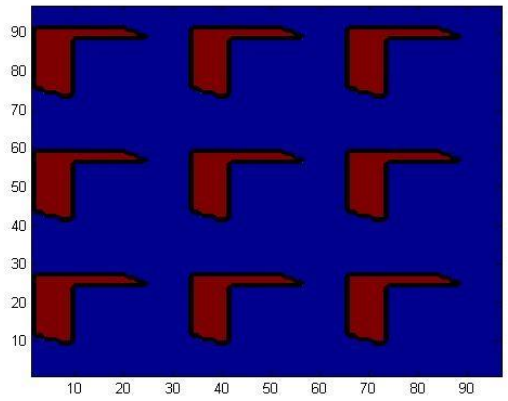

Figure 8: Shade modeling example

Red area indicates shade area, blue is sunlit area. This example proves that in 1000

am PST in June 22nd of San Diego, CA, USA. Shadow accumulates on western area of a building and also covers a small area on north of the building.

3.3.2. Long wave radiation from the atmosphere

Sky long wave radiation describes the radiation emitted from atmosphere. A demonstrated equation, Angstrom formula [46], is commonly used. The contribution of long wave radiation from sky to the MRT need to be weighted by the sky view factor. Sky view factor (SVF) indicates the ratio between radiation received by a planar surface and that from the entire hemispheric radiating environment [47]. The SVF is calculated as the fraction of sky visible when viewed from the ground up. Wu [48] introduces a calculation method of SVF estimation in urban area, which we found is the most suitable in this paper. It starts with calculating the wall view factor (WVF) using the azimuths (γ) and altitude (β) angles to the building. The Algorithm of SVF is shown as below. A modeling example of SVF (Canyon Aspect ratio is 1/2) presents in Figure 9.

$$WVF_{M2} = \frac{1}{2\pi}\{(\gamma_2 - \gamma_1) + cos\beta[tan^{-1}(cos\beta tan\gamma_1) - tan^{-1}(cos\beta tan\gamma_2)]\} \quad (28)$$

and

$$SVF_{ref-M2} = 1 - (WVF_{1-M1} + WVF_{2-M2}) \quad (29)$$

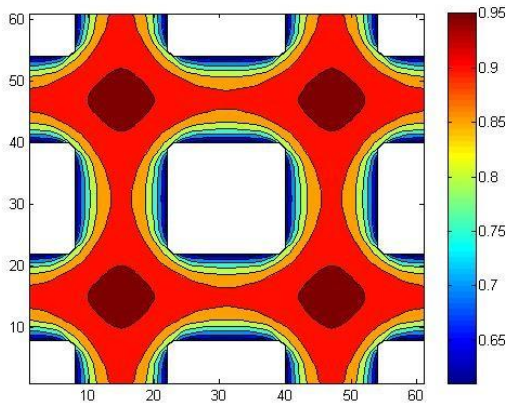

Figure 9: Sky view factor modeling result

3.3.3. Long wave radiation from building and ground

The third term describes long wave radiation from building and ground surfaces. It is a sum of visible surface temperature; each was weighted by view factor. In this paper, surface temperature data (ground temperature and building wall surface temperature) is obtained from [25]. View factor is the proportion of radiation which release from surface A and strikes surface B. By using the matrix-based model, it is easy to analysis view factor between each two different spot in the 3D idealized model. View factor equations are available in most of thermal comfort textbooks [49, 28].

Before calculating the long wave radiation, there is one more problem remained. Imagine a person stand in the middle of the urban area, apparently not every point in the area is visible to the person, which means not every point in the area can generates long wave radiation to the analyzing point. Part of the long wave radiation would be blocked by objects, such as buildings. Therefore, visibility modeling is important to the long wave radiation modeling. A algorithm is developed in this paper to model the visibility, shown as follow:

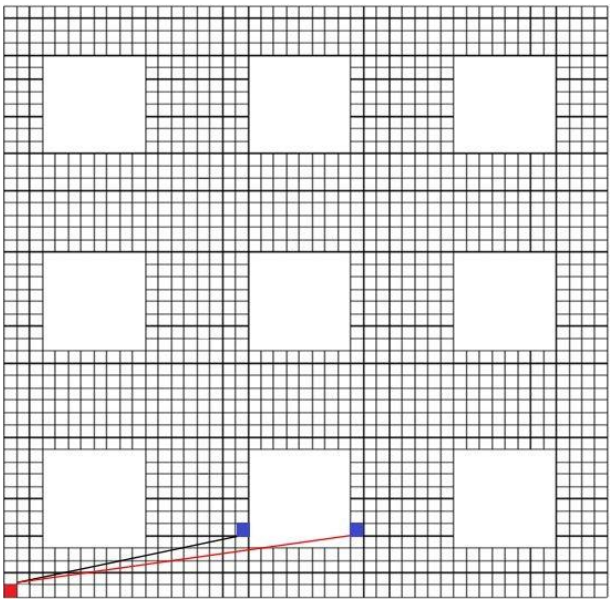

Figure 10: Visibility test description

First, make a line between two different urban ground surfaces (elements of the ground matrix) and check if the line has intersection with project of any one of the buildings. If yes, the current two pieces of ground surface are visible to each other. Otherwise, it is not. For each analyzing point, a ground visibility matrix has generated and stored. Shown in the Figure 10, Red dot donates people standing location, blue dot donates testing surface. Red line means invisible. Black line means visible:

Here are some visibility modeling examples, each respect to analyzing point at (30, 30); (30, 50) and (15, 90). In order to show the visibility better, these three examples are generated with smaller building size than the actual data used in this paper:

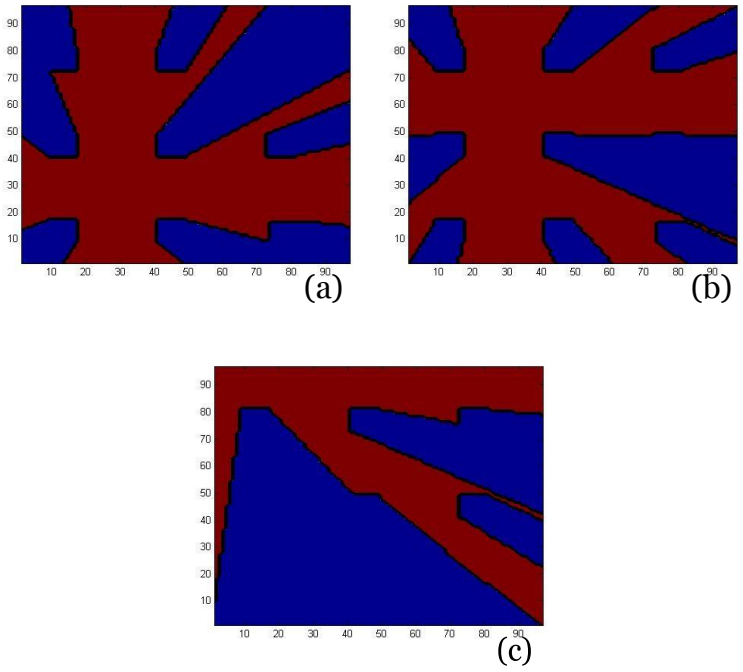

Figure 11: Visibility modeling examples

Second, after finished checking the urban ground surfaces visibility, visibility of building side surfaces could be known by checking visibility on surrounding ground surfaces of each building. For each analyzing point, 9 building surface visibility matrices are generated and stored. Shown in Figure 12:

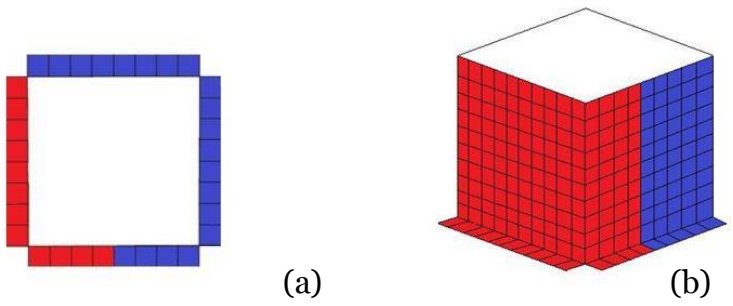

Figure 12: Wall surface visibility modeling

Chapter 2, Chapter 3, Chapter 4 and Chapter 5, in part, is a reprint of the material as it appears in "A New Numerical Simulation Model for Standard Effective Temperature", Jipeng Fan, Negin Nazarian, Jan Kleissl. The dissertation author was the primary investigator and author of this paper.

4. Simulation Results

4.1. Time Changing Spatial SET Distribution

Results of this paper are calculated under a series of assumptions on human thermal comfort properties. The testing subject is assumed to be a 173 cm height, 70 kg weight male, wearing typical summer clothes, standing in the enter area of San Diego, California, USA in a clear summer day. Analyzing level is on pedestrians' level (1.5 meters from ground). Average wind velocity, in the domain, is about 2 m/s. Canyon aspect ratio is 1. We first studied time changing spatial SET distribution. Each of them runs at Neutral (no solar radiation), PST 0600, PST 0800, PST 1000, PST 1200, PST 1400, PST 1600, PST 1800. Instantaneous ground temperature distribution presents as reference.

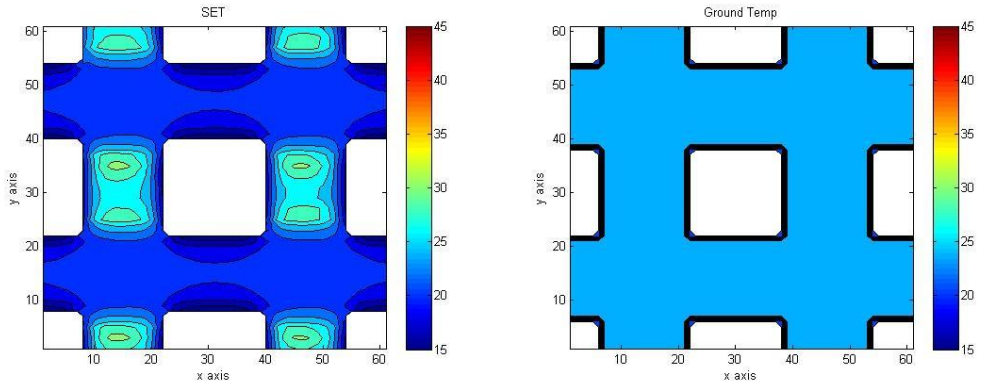

(a) SET (b) Ground Temperature

Figure 13: SET distribution at Neutral

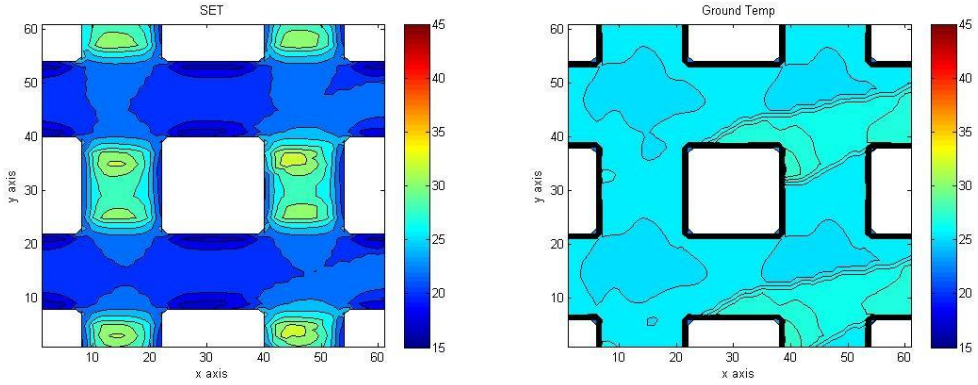

(a) SET (b) Ground Temperature

Figure 14: SET distribution at 0600 PST

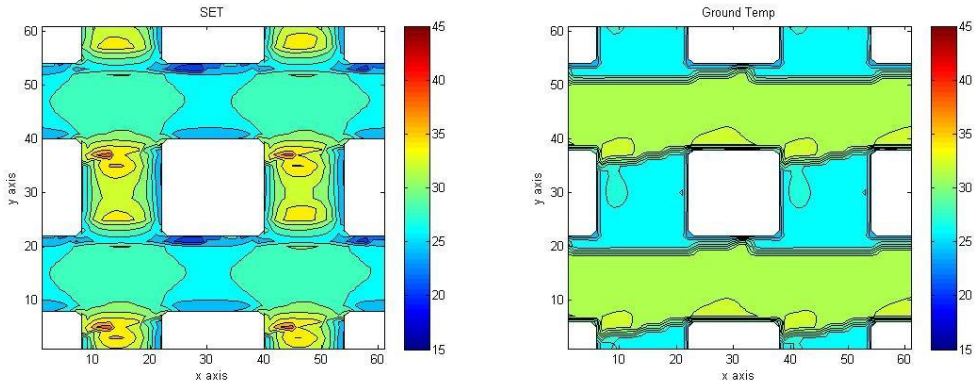

(a) SET (b) Ground Temperature

Figure 15: SET distribution at 0800 PST

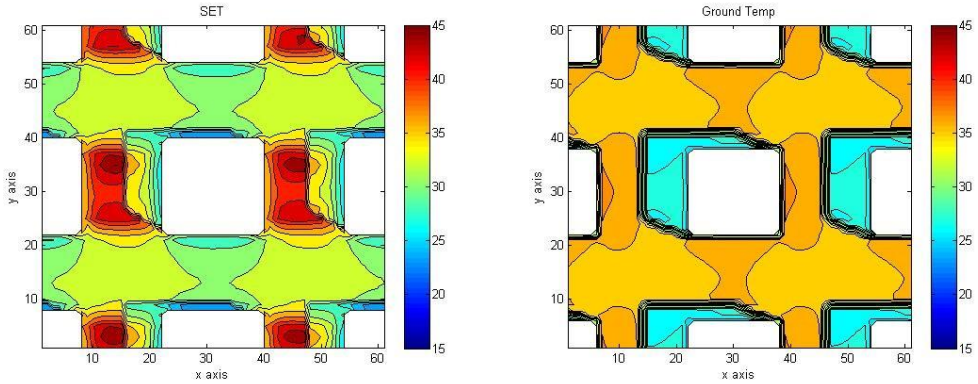

(a) SET (b) Ground Temperature

Figure 16: SET distribution at 1000 PST

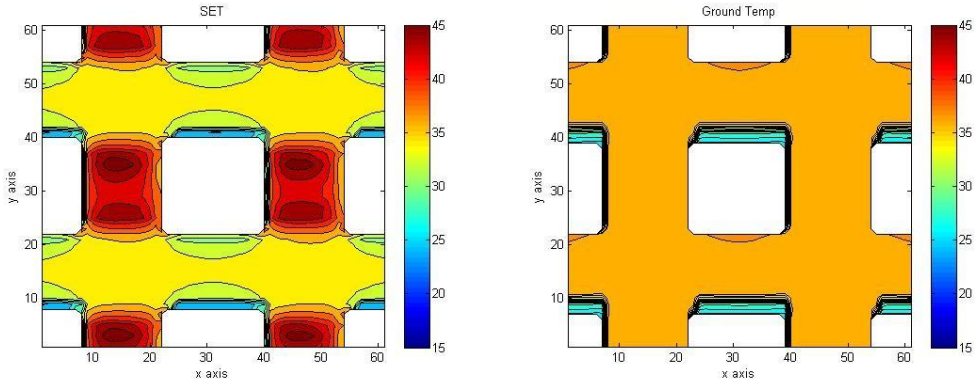

(a) SET (b) Ground Temperature

Figure 17: SET distribution at 1200 PST

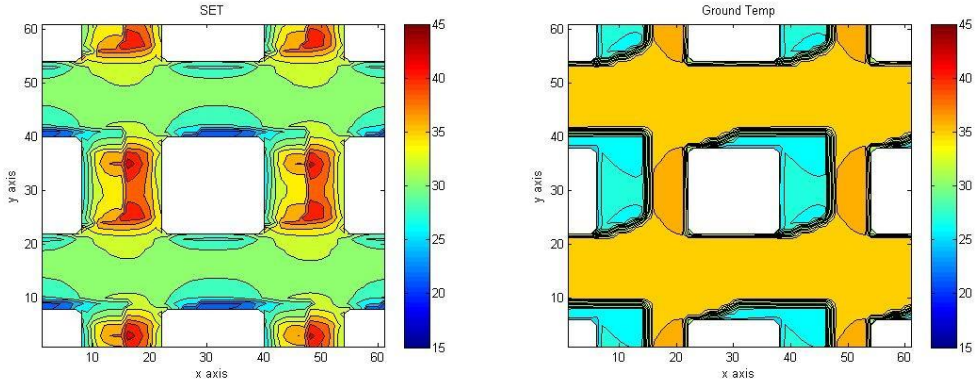

(a) SET (b) Ground Temperature

Figure 18: SET distribution at 1400 PST

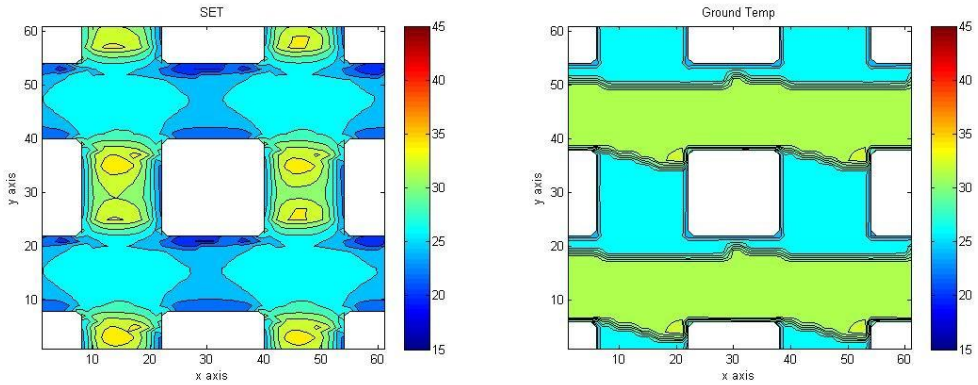

(a) SET (b) Ground Temperature

Figure 19: SET distribution at 1600 PST

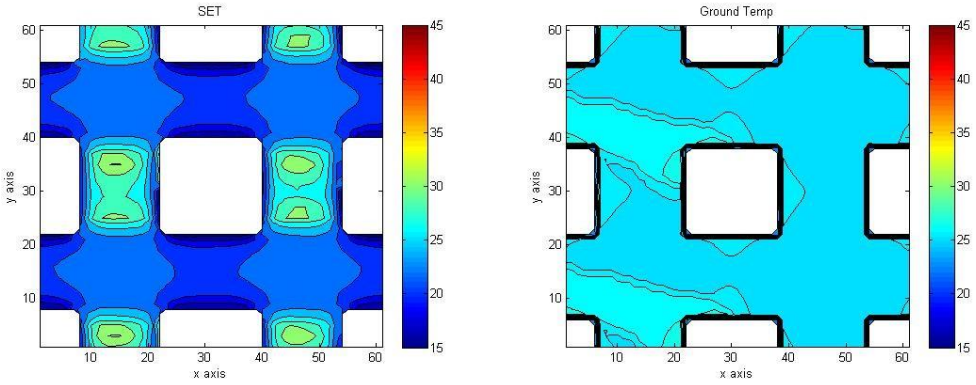

(a) SET (b) Ground Temperature

Figure 20: SET distribution at 1800 PST

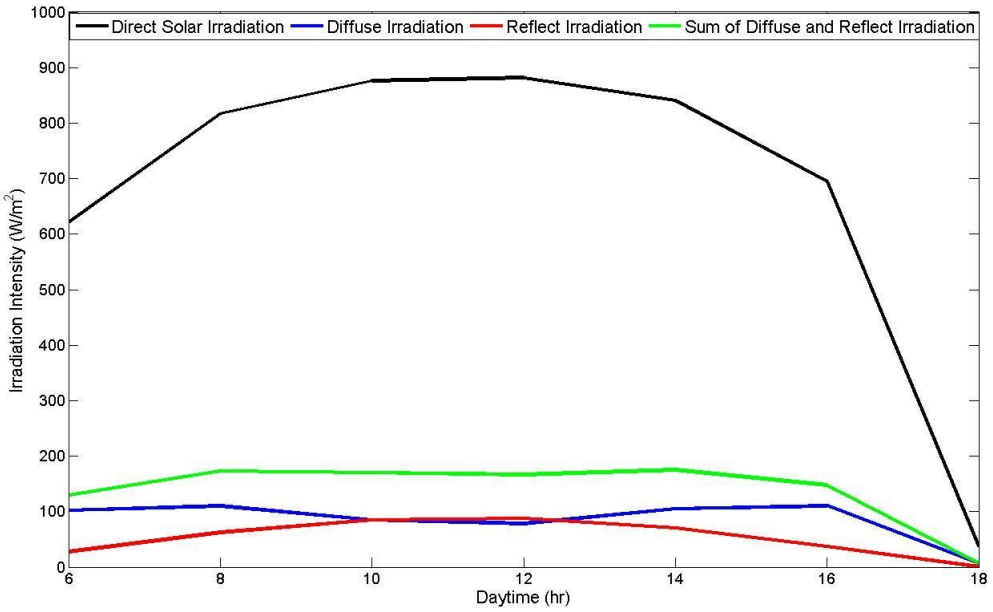

Figure 21: Solar intensity change during a day

The result have shown that SET change greatly even in a small area. Figure 21 describes changing of each of three terms of solar radiation. It shows that the solar peak occurs at 1200 PST in a day. Before 1200 PST during the daylight, solar radiation intensity increased monotonically. After 120 PST, solar radiation intensity decreased monotonically until sunset. Same change regulation also presents in SET distribution plots as both MRT and air temperatures are changed with solar radiation

intensity. In Figure 15, 16, 17, 18 and 19, how a shade effects SET is clearly shown. During these hours, the rate of sum of diffuse and reflection radiation to total solar radiation is higher than other testing cases (21). This makes shade has bigger effect on SET as diffuse and reflection radiation only occur in sunlit area. However, the shade effect is a complex consequence rather than a simple causation of solar intensity. While solar intensity remain constant effect on the short wave radiation (term 1 of Equation 27), long wave radiation (term 2 of Equation 27) is also changing because temperature of urban ground and building surfaces are changing (co-effected by solar radiation and wind), short wave radiation (term 3 of Equation 27) is changing with air temperature which is also effected by solar intensity. Therefore, this research come out a conclusion on shade effect of SET which is that shade can has significant effect on SET depends on time in a day but their categorical changing regulation might have to be determined for each individual cases. The special SET plots also indicate that spacious space obtains higher SET during heavy solar intensity hours. Known from the sky view factor plot (Figure 9), higher short wave radiation from sky could be received in spacious space (cross section).

Figure 22 is a time changing SET distribution which set up on a line in urban area, line location shown as Figure 24(a). Figure 23 is a time changing SET distribution which set up on a loop in urban area, line location shown as Figure 24(b). From Figure 22, in sunlit area, the largest difference between maximum and minimum SET is changing along the day time changing and no larger than 2 degrees. Figure 22 indicates that SET increases significantly at span-wise canyon.

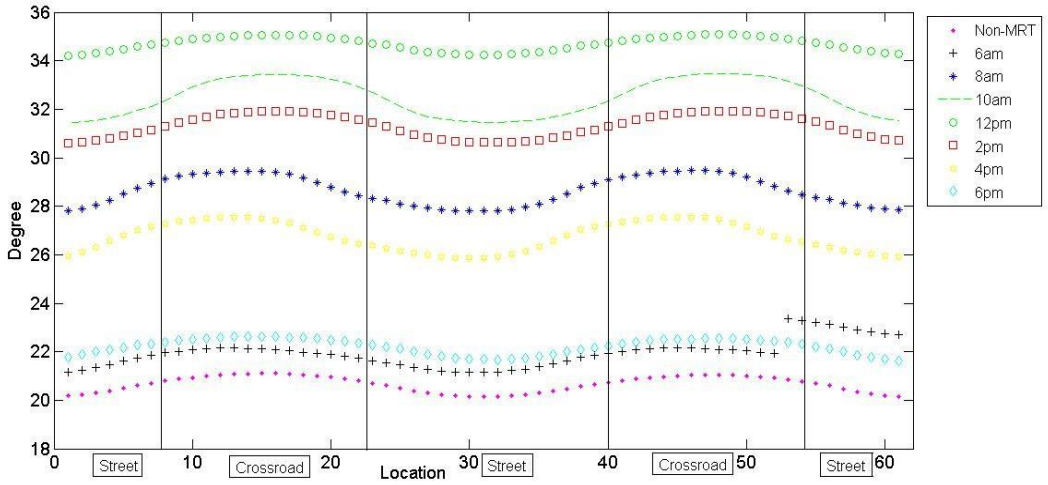

Figure 22: SET distribution in a line

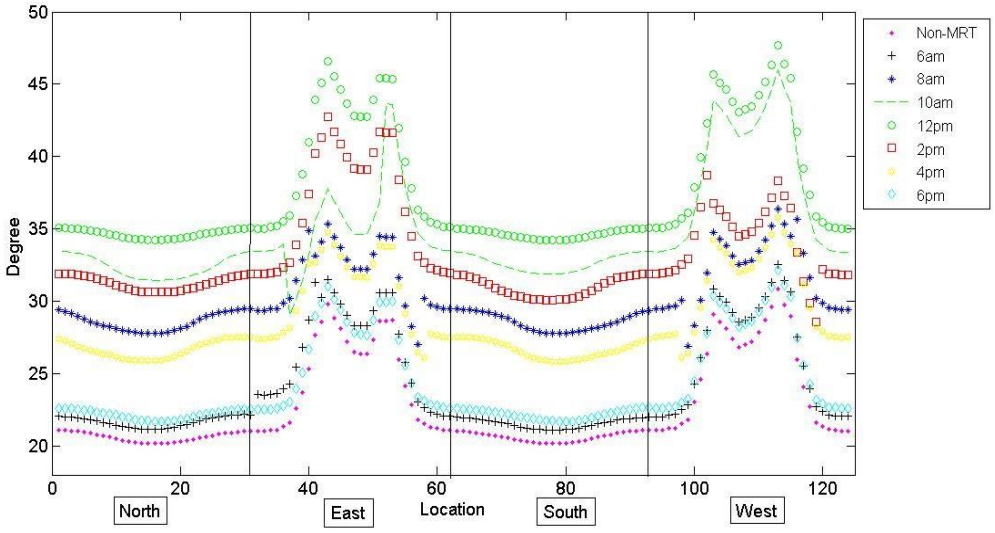

Figure 23: SET distribution on a circle

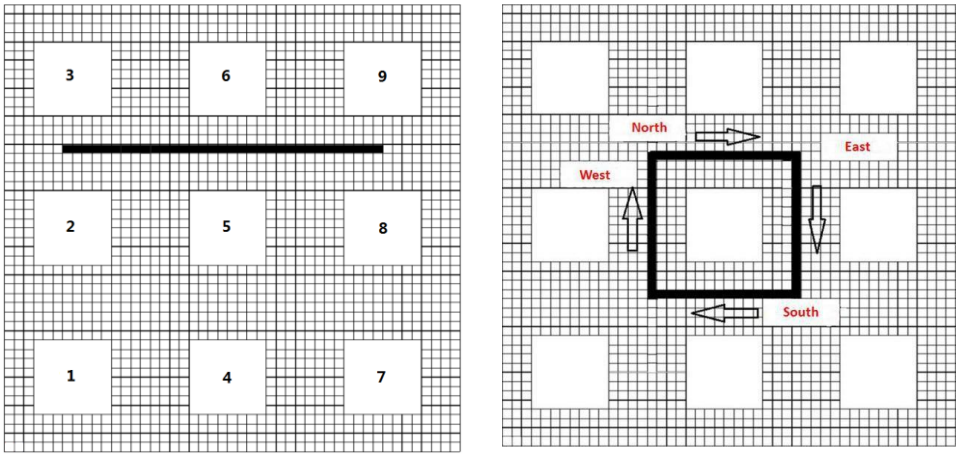

(a) Line test set up (b) Loop test set up

Figure 24: Test location set up

4.2. Wind Direction Changing Spatial SET Distribution

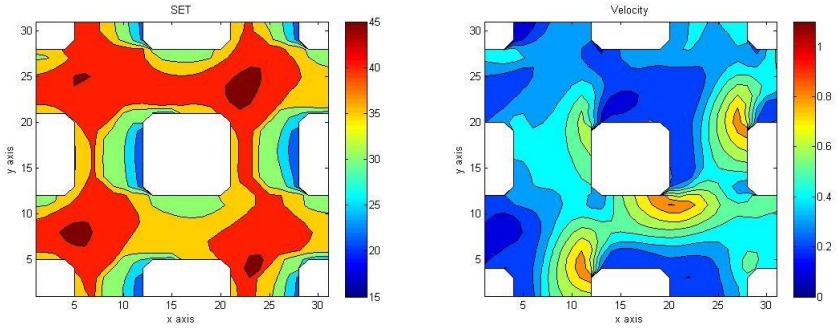

(a) SET (b) Wind Velocity

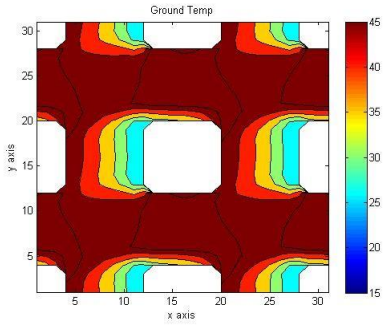

(c) Ground Temperature

Figure 25: Wind blow from northwest

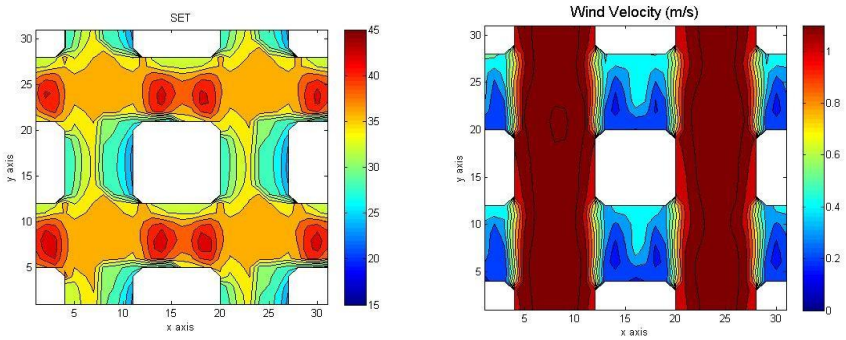

(a) SET (b) Wind Velocity

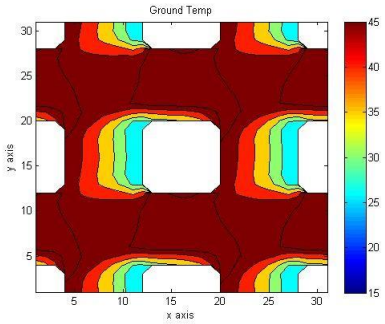

(c) Ground Temperature

Figure 26: Wind blow from south

According to Figure 26, wind direction is not a variable of SET. Since wind direction can change the building wall temperature distribution [25] and urban temperature distribution is one of the major parameters of MRT. Therefore, it is valuable to analyze the effect of wind direction to SET distribution. Upon plots show that results of wind blow from 45 degrees and 90 degrees at PST 1000am. If compare figure 26 with 16, a conclusion comes out easily which is the wind direction does not play a significant role in thermal comfort. In fact, wind direction is not a dominant force to the MRT before each term of the MRT should be weighted by view factor. By calculation, wall surface view factor and ground view factor are not on same order of magnitudes. For most part of standing location in the urban area, sum of ground view factor is hundreds times of the wall view factor. After weighted by view factor,

effect of wind direction to SET distribution is negligible.

4.3. Canyon Aspect Ratio Changing Spatial SET Distribution

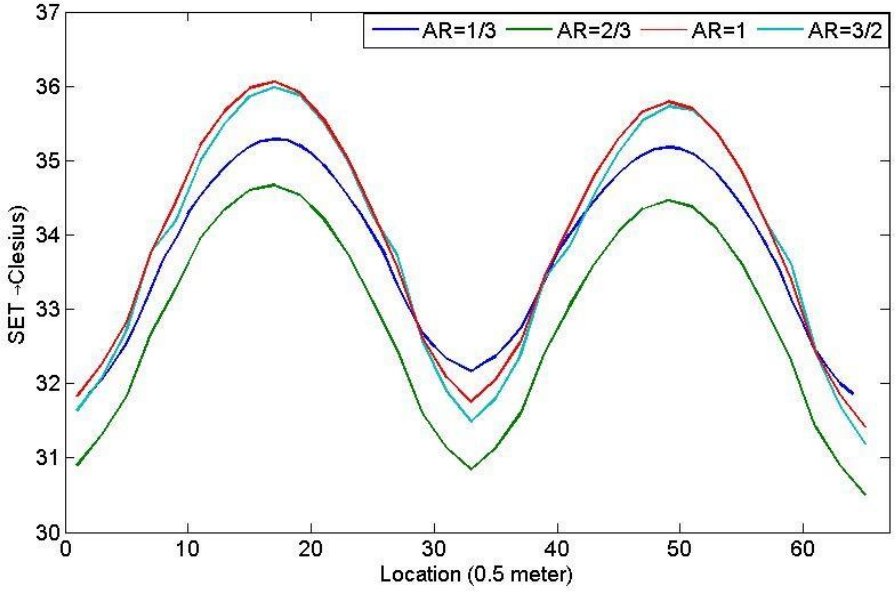

Figure 27: SET distribution changing with Canyon Aspect Ratio

Regard to the goal of this paper, a urban planner might able to read follow information about idealized 3D urban model: First, effect of shade to the city thermal comfort changing along time in a day. This is because shade can only block the direct solar radiation. Contribution of direct solar radiation to total is changing. Second, SET does not monotone increasing with canyon aspect ratio. Canyon aspect ratio is a common geometry parameter to urban planners. It is studied, results shown in 27, as a single one controlled variable in this paper. It makes complex consequence to the SET because it costs different effects, both positive and negative, to SET variables. 27 indicates that, for the current building material and design setup, SET is lower at 2/3 AR at the PST 10 am. In fact, variables that can cost complex effect to SET is common in this study. In order to have a better thermal comfort urban area design, this simulation should be run for multiple times to check each possible design.

Chapter 2, Chapter 3, Chapter 4 and Chapter 5, in part, is a reprint of the material as it appears in "A New Numerical Simulation Model for Standard Effective Temperature", Jipeng Fan, Negin Nazarian, Jan Kleissl. The dissertation author was the primary investigator and author of this paper.

5. Conclusions and Future Perspectives

In this paper, we built a urban matrix model, simulated radiation as MRT in urban area and developed a new numerical model to simulate the SET in a idealized 3x3 buildings urban matrix. The major different of this study with previous researches is it allows to simulate the urban thermal comfort without experimental tests. Through this study, it is expected that more effective thermal comfort reference to urban or building designs. Some existed researches are able to predict the SET, like CityComfort+ [21], Rayman [20], ENVI-met [19], and SOLWEIG [22]. Through this study, we can provide more stimulative methods and model for reference and to make up the functional insufficiency of these methods. This model is still under developed. The next step is to compare stimulative results with experimental tests. This model could be further improved by compare its performance with other SET prediction methods. In order to apply this model to a real urban geographic area. More complicate MRT simulation need to be develop, such as: view factor, sky view factor and shade calculation for complex geometry buildings.

Chapter 2, Chapter 3, Chapter 4 and Chapter 5, in part, is a reprint of the material as it appears in "A New Numerical Simulation Model for Standard Effective Temperature", Jipeng Fan, Negin Nazarian, Jan Kleissl. The dissertation author was the primary investigator and author of this paper.

6. Bibliography

[1]UN Desa. World urbanization prospects, the 2014 revision. *New York:United Nations Department of*, 2015.

[2]HH Kim. Urban heat island. *International Journal of Remote Sensing*, 13(12):2319–2336, 1992.

[3]Tim R Oke. Canyon geometry and the nocturnal urban heat island: comparison of scale model and field observations. *Journal of climatology*, 1(3):237–254, 1981.

[4]Tim R Oke City size and the urban heat island. *Atmospheric Environment (1967)*, 7(8):769–779, 1973.

[5]Robert D Bornstein. Observations of the urban heat island effect in New York City. *Journal of Applied Meteorology*, 7(4):575–582, 1968.

[6]Jianguo Tan, Youfei Zheng, Xu Tang, Changyi Guo, Liping Li, Guixiang Song, Xinrong Zhen, Dong Yuan, Adam J Kalkstein, Furong Li, et al. The urban heat island and its impact on heat waves and human health in shanghai. *International journal of biometeorology*, 54(1):75–84, 2010.

[7]CP Lo and Dale A Quattrochi. Land-use and land-cover change, urban heat island phenomenon, and health implications. *Photogrammetric Engineering & Remote Sensing*, 69(9):1053–1063, 2003.

[8]Anna Mavrogianni, Michael Davies, M Batty, SE Belcher, SI Bohnenstengel, David Car- ruthers, Z Chalabi, B Croxford, C Demanuele, S Evans, et al. The comfort, energy and health implications of london's urban heat island. *Building Services Engineering Research and Technology*, page 0143624410394530, 2011.

[9]Ken Parsons.*Human thermal environments: the effects of hot, moderate, and cold environments on human health, comfort, and performance*. Crc Press, 2014.

[10]T Oohori, LG Berglund, and AP Gagge. Comparison of current two-parameter indices of vapor permeation of clothing: as factors governing thermal equilibrium and human comfort. *ASHRAE transactions*, 90(2):85–101, 1984.

[11]Guodong Ye, Changzhi Yang, Youming Chen, and Yuguo Li. A new approach for mea-suring predicted mean vote (pmv) and standard effective temperature (set). *Building and Environment*, 38(1):33–44, 2003.

[12]Tsuyoshi Honjo. Thermal comfort in outdoor environment. *Global environmental research*, 13(2009):43–47, 2009.

[13]Kentaro Aoyama, Sae Kyogoku, Sintaro Nakayama, Rieko Yagi, Hideki Takebayashi, Et- suko Ishii, Makiko Kasahara, Shingo Tanabe, and Makoto Kouyama. Evaluation of the outdoor thermal environment in redevelopment buildings in front of osaka station based on observations. *Journal of Heat Island Institute International Vol*, 9:2, 2014.

[14]Jordi Mazon. The influence of thermal discomfort on the attention index of teenagers: an experimental evaluation. *International journal of biometeorology*, 58(5):717–724, 2014.

[15]Lilly Rose, Ebin Horrison, and Lavanya Jothi Venkatachalam. Influence of built form onthe thermal comfort of outdoor urban spaces.

[16]Richard W Katz and Barbara G Brown. Extreme events in a changing climate: variability is more important than averages. *Climatic change*, 21(3):289–302, 1992.

[17]Bhupendra Nath Goswami, V Venugopal, D Sengupta, MS Madhusoodanan, and Prince KXavier. Increasing trend of extreme rain events over india in a warming environment. *Science*, 314(5804):1442–1445, 2006.

[18]Tyler Hoyt, Stefano Schiavon, Alberto Piccioli, Dustin Moon, and Kyle Steinfeld. Cbe thermal comfort tool. *Center for the Built Environment, University of California Berkeley, http://cbe. berkeley. edu/comforttool*, 2013.

[19]Michael Bruse. Envi-met 3.0: updated model overview. University of Bochum Retrieved from: www.envimet.com, 2004.

[20]Andreas Matzarakis, Frank Rutz, and Helmut Mayer. Modeling radiation fluxes in simple and complex environments—application of the rayman model. *International Journal of Biometeorology*, 51(4):323–334, 2007.

[21]Jianxiang Huang, Jose Guillermo Cedeno-Laurent, and John D Spengler. Citycomfort+: A simulation-based method for predicting mean radiant temperature in dense urban areas. *Building and Environment*, 80:84–95, 2014.

[22]Fredrik Lindberg, Björn Holmer, and Sofia Thorsson. Solweig 1.0–modeling spatial variations of 3d radiant fluxes and mean radiant temperature in complex urban settings. *Inter- national Journal of Biometeorology*, 52(7):697–713, 2008.

[23]Fazia Ali Toudert. Dependence of outdoor thermal comfort on street design in hot and dry climate.

[24]Sofia Thorsson, Fredrik Lindberg, Ingegärd Eliasson, and Björn Holmer. Different methods for estimating the mean radiant temperature in an outdoor urban setting. *International Journal of Climatology*, 27(14):1983–1993, 2007.

[25]N Nazarian and JP Kleissl. Effects of non-uniform wall heating on thermal and momentum fields in a 3-dimensional urban environment. In *AGU Fall Meeting Abstracts*, volume 1, page 0316, 2014.

[26]AP Gagge, Y Nishi, and RR Gonzalez. Standard effective temperature-a single temperature index of temperature sensation and thermal discomfort. In *Proceedings of the CIB Commission W45 (human requirements) symposium held at the Building Research Station*, pages 229–50, 1972.

[27]Delafield Du Bois and Eugene F Du Bois. Clinical calorimetry: tenth paper a formula to estimate the approximate surface area if height and weight be known. *Archives of internal medicine*, 17(6_2):863–871, 1916.

[28]ASHRAE Handbook Fundamentals. American society of heating, refrigerating and air conditioning engineers. *Inc., NE Atlanta, GA*, 30329, 2009.

[29]Margaret H Hardy. The development in vitro of the mammary glands of the mouse. *Journal of anatomy*, 84(Pt 4):388, 1950.

[30]AP Gagge, GM Rapp, and JD Hardy. The effective radiant field and operative temperature necessary for comfort with radiant heating. *ASHRAE Trans*, 73(1):121–129, 1967.

[31]AJH Vendrik and JJ Vos. A method for the measurement of the thermal conductivity of human skin. *Journal of Applied Physiology*, 11(2):211–215, 1957.

[32]BW Olesen, E Sliwinska, TL Madsen, and PO Fanger. Effect of body posture and activity on the thermal insulation of clothing: Measurements by a movable thermal manikin. *ASHRAE transactions*, 88:791–805, 1982.

[33]PO Fanger. Calculation of thermal comfort, introduction of a basic comfort equation. *ASHRAE transactions*, 73(2):III–4, 1967.

[34]E Lehtinen and S Seppänen. Side effects of conray meglumin 282 and dimer-x in lumbar myelography. *Acta Radiologica Diagnosis (Sweden)*, 12(1):12–16, 1972.

[35]Alan H Woodcock. Moisture transfer in textile systems, part i. *Textile Research Journal*, 32(8):628–633, 1962.

[36]LARRY G Berglund and RICHARD R Gonzalez. Evaporation of sweat from sedentary man in humid environments. *Journal of Applied Physiology*, 42(5):767–772, 1977.

[37]NZ Azer. Design guidelines for spot cooling systems: Part 1. assessing the acceptability of the environment. *ASHRAE Trans.;(United States)*, 88(CONF-820112-), 1982.

[38]Elizabeth A McCullough, Byron W Jones, and Janice Huck. *A comprehensive data base for estimating clothing insulation*. Citeseer, 1985.

[39]GIANFRANCO Rizzo, G Franzitta, and G Cannistraro. Algorithms for the calculation of the mean projected area factors of seated and standing persons. *Energy and buildings*, 17(3):221–230, 1991.

[40]PO Fanger. Thermal comfort: analysis and applications in environmental engineering, by PO Fanger, 1972.

[41]A Pharo Gagge, AP Fobelets, and LoG Berglund. A standard predictive index of human response to the thermal environment. *ASHRAE Trans.;(United States)*, 92(CONF-8606125-),1986

[42]Francesca Romana d'Ambrosio Alfano, Marco Dell'Isola, Boris Igor Palella, Giuseppe Riccio, and Aldo Russi. On the measurement of the mean radiant temperature and its influence on the indoor thermal environment assessment. *Building and Environment*, 63:79–88, 2013.

[43]Stephan D Flint and Martyn M Caldwell. Solar uv-b and visible radiation in tropical forest gaps: measurements partitioning direct and diffuse radiation. *Global change biology*, 4(8):863–870, 1998.

[44]Parameswaran Sreekumar, DL Bertsch, BL Dingus, JA Esposito, CE Fichtel, RC Hartman,SD Hunter, G Kanbach, DA Kniffen, YC Lin, et al. Egret observations of the extragalactic gamma-ray emission. *The Astrophysical Journal*, 494(2):523, 1998.

[45]Sasha Madronich and Siri Flocke. The role of solar radiation in atmospheric chemistry. In *Environmental photochemistry*, pages 1–26. Springer, 1999.

[46]Anders Knutsson Ångström. *A study of the radiation of the atmosphere: based upon observa- tions of the nocturnal radiation during expeditions to Algeria and to California*, volume 65. Smithsonian Institution, 1915.

[47]Marie K Svensson. Sky view factor analysis–implications for urban air temperature differ- ences. *Meteorological applications*, 11(03):201–211, 2004.

[48]Jie WU, Yufeng ZHANG, and Qinglin MENG. Calculation method of sky view factor based on rhino-grasshopper platform. In *13th Conference of International Building Performance Simulation Association, Chambery, France, August 26*, volume 28, page 2013, 2013.

[49]Poul O Fanger et al. Thermal comfort. analysis and applications in environmental engi- neering. *Thermal comfort. Analysis and applications in environmental engineering.*, 1970.